

Journal of Mechanics of Materials and Structures

**INTERFACIAL WAVES IN AN A/B/A PIEZOELECTRIC STRUCTURE WITH
ELECTRO-MECHANICAL IMPERFECT INTERFACES**

M. A. Reyes, J. A. Otero and R. Pérez-Álvarez

Volume 12, No. 4

July 2017



INTERFACIAL WAVES IN AN A/B/A PIEZOELECTRIC STRUCTURE WITH ELECTRO-MECHANICAL IMPERFECT INTERFACES

M. A. REYES, J. A. OTERO AND R. PÉREZ-ÁLVAREZ

We study the propagation of shear horizontal (SH) waves in the interfaces of an A/B/A piezoelectric structure with an electrical and mechanical imperfect contact, being modeled by means of a capacitor and a spring, respectively. The analytical dispersion relations are obtained and some limit cases are analyzed in detail, predicting the existence of interface waves. Based on numerical calculations, it can be shown that the electrical and mechanical imperfections strongly influence the dispersion curves.

1. Introduction

The possibility of an elastic shear surface wave being guided by the free surface of a piezoelectric crystal with 6 mm hexagonal symmetry has been studied in [Bleustein 1968].

Maerfeld and Tournois [1971] found that these kinds of waves can also be guided by the interface in perfect contact between two semi-infinite media, where at least one of these is a piezoelectric medium. Moreover, a shear horizontal (SH) wave propagating along an interface between a piezoelectric half-space and piezomagnetic half-space was investigated in [Soh and Liu 2006]. In [Fan et al. 2006b], imperfection was considered by means of a discontinuity of the displacement (spring model). An exact solution for antiplane waves in a ceramic half-space including an imperfectly bonded layer was obtained in [Fan et al. 2006a]. In [Chen et al. 2008], an exact solution for antiplane waves in a 6 mm crystal between two piezoceramic half-spaces with imperfect interface bonding was obtained. Furthermore, the effect of an electric field gradient on the SH interface waves was investigated in [Yang and Yang 2009]. The SH surface waves propagating in a layered piezoelectric half-space with an imperfectly bonded interface were studied in [Liu et al. 2010]. In [Sun et al. 2011], the SH wave propagation was studied in a cylindrical PE/PM structure with an imperfect interface and two exact dispersion relations were obtained. Dispersion relations of SH waves in an A/B/A heterostructure (which has different magnetic, electric and elastic properties with imperfect bonding at the surfaces) taking 6 mm hexagonal symmetry into account have been studied in great detail by Otero et al. [2011], giving some dispersion curves for different A/B/A heterostructures with magneto-electro-elastic properties and showing how strongly the behavior of these curves depends on the spring constant material parameter k_u (GPa/m). In [Otero et al. 2012], propagation of SH waves between the interfaces of two piezoelectric materials with electro-mechanical imperfect contacts modeled by means of a spring and a capacitor and the corresponding dispersion relations for the imperfect contact was presented.

Several works have been presented in order to study the effects of interface bonding on acoustic wave generation in elastic bodies using piezoelectric transducers driven electrically, as in [Li et al. 2013].

Keywords: piezoelectricity, dispersion curve, wave propagation, imperfect contact.

A coupling model for interfacial imperfection is proposed in [Li et al. 2015a] in order to characterize the imperfect interface in a bilayered multiferroic cylinder, and in [Li et al. 2016a] the SH wave propagation at the interface in a bilayered multiferroic is considered. In [Li and Jin 2015], the shear-lag interface model is used to simulate the effect of an imperfect interface on SH wave propagation in a piezoelectric composite structure. Trying to generalize the interfacial imperfection coupling model, Li et al. [2015b] introduced a new model to describe the magneto-electro-mechanical imperfect interfacial region in a multiferroic composite consisting of an FE layer and another FM layer. Xiong et al. [2015] proposed an interfacial sliding prevention/promotion model in order to consider the effect of interfacial normal stress on interfacial sliding and Li et al. [2015c; 2016b] proposed a generalization of the spring model while including intercoupling effects. Some authors, like Kakar [2015], have investigated the existence of SH waves in a fiber-reinforced layer placed over a heterogeneous elastic half-space. Kong et al. [2016] studied the propagation of SH waves in the layered structure consisting of a transversely isotropic FGPM layer and a PMN-0.29PT substrate that is being poled along [011]_c, finding that the dispersion characteristics of the SH waves are dominated by the cut orientation of the PE substrate.

In the present work, different to the work of Otero et al. [2011], we consider the existence of two imperfections at the interfaces on an A/B/A piezoelectric structure: electrical and mechanical. The presence of electrical and mechanical imperfections are modeled by means of a capacitor and a spring, respectively. The capacity of the capacitor is the measure of the electrical imperfection.

This paper is organized as follows: in Section 2 the equations governing the SH wave propagating in piezoelectric materials with 6 mm hexagonal symmetry and the constitutive relations are presented. Section 3 is dedicated to the general formulation of the main problem, considering two types of imperfections at the interfaces. Symmetric and antisymmetric solutions are obtained for a specific system. Section 4 is devoted to calculating the dispersion relations, and some limiting cases are analyzed. These results are in agreement with known results from the literature. In Section 5 some numerical examples are shown and analyzed. Finally, in Section 6 some conclusions are presented.

2. Governing equations for the SH mode

A system of two coupled partial differential equations with two unknowns: the z component of the elastic displacement u_z and the in-plane electric potential φ , describe SH waves in this type of material; that is,

$$c\nabla^2 u + e\nabla^2 \varphi = \rho \frac{\partial^2 u}{\partial t^2}, \quad (2-1)$$

$$e\nabla^2 u - \varepsilon\nabla^2 \varphi = 0, \quad (2-2)$$

where $\nabla^2 \equiv \partial^2/\partial x^2 + \partial^2/\partial y^2$ and $u \equiv u_z$. Here, $c \equiv c_{44}$, $e \equiv e_{15}$, $\varepsilon \equiv \varepsilon_{11}$ are the elastic, piezoelectric, and dielectric permittivity coefficients, respectively. For the case of SH waves, both components u_x and u_y are equal to zero. Equations (2-1)–(2-2), which depend only on (x, y, t) , describe the motion of a SH wave in a homogeneous material. Firstly, we have to rewrite (2-1)–(2-2) using an auxiliary potential function ϕ defined by

$$\phi = \varphi - \frac{e}{\varepsilon} u. \quad (2-3)$$

Then, (2-1) can be written as

$$\left(\nabla^2 - \frac{1}{\bar{v}^2} \frac{\partial^2}{\partial t^2}\right)u = 0, \tag{2-4}$$

where $\bar{v} = \sqrt{\bar{c}/\rho}$ is the bulk shear wave speed within the piezoelectric and $\bar{c} = c + e^2/\varepsilon$ is the electro-elastically stiffened constant. Secondly, (2-2) can be written as

$$\nabla^2\phi = 0. \tag{2-5}$$

3. SH waves in piezoelectrics

Consider a piezoelectric material with 6 mm hexagonal symmetry exhibiting polarization in the z -axis direction of an xyz Cartesian coordinate system and the xy plane is an isotropy plane. The planes $y = \pm\frac{1}{2}d$ are the interfaces. The spaces $y < -\frac{1}{2}d$ and $y > \frac{1}{2}d$ are occupied by a piezoelectric of type A and the region enclosed in the interval $[-\frac{1}{2}d, \frac{1}{2}d]$ by a piezoelectric of type B, as shown in Figure 1.

We want to find u and ϕ describing SH waves propagating along the positive x axis that satisfy (2-4) and (2-5) at each interface of the piezoelectric structure. We are really interested in finding confined modes, which is why the functions u and ϕ in media A should vanish as y goes to $\pm\infty$. This in turn implies that at these interfaces the solutions of (2-4) and (2-5) must be of the form

$$u_s = e^{i(\xi x - \omega t)} \begin{cases} U_A e^{\eta_A y} & \text{if } y < -\frac{1}{2}d, \\ U_B \cos(\eta_B y) & \text{if } |y| \leq \frac{1}{2}d, \\ U_A e^{-\eta_A y} & \text{if } y > \frac{1}{2}d, \end{cases} \tag{3-1}$$

for the symmetric modes in y , and

$$u_{as} = e^{i(\xi x - \omega t)} \begin{cases} U_{A1} e^{\eta_A y} & \text{if } y < -\frac{1}{2}d, \\ U_{B1} \sin(\eta_B y) & \text{if } |y| \leq \frac{1}{2}d, \\ -U_{A1} e^{-\eta_A y} & \text{if } y > \frac{1}{2}d, \end{cases} \tag{3-2}$$

for the antisymmetric modes in y , where U_A , U_B , U_{A1} , and U_{B1} are undetermined constants. Here, ω , ξ , and η are the frequency, the x -component of the wave vector, and the y -component of the wave vector,

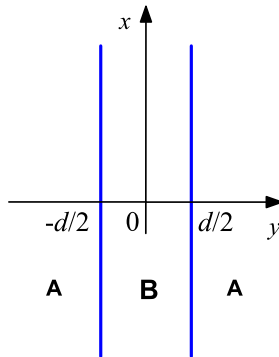


Figure 1. Scheme of a piezoelectric structure A/B/A.

respectively, which are related to each other through the expressions

$$\begin{aligned} \eta_A &= \xi \sqrt{(1 - v^2/\bar{v}_A^2)} > 0, \quad |y| \geq \frac{1}{2}d, \\ \eta_B &= \xi \sqrt{(v^2/\bar{v}_B^2 - 1)} > 0, \quad |y| \leq \frac{1}{2}d, \end{aligned} \tag{3-3}$$

where $v = \omega/\xi$ is the phase velocity. Using the above considerations, we obtain

$$\phi_s = e^{i(\xi x - \omega t)} \begin{cases} \Phi_A e^{\xi y} & \text{if } y < -\frac{1}{2}d, \\ \Phi_B \cosh(\xi y) & \text{if } |y| \leq \frac{1}{2}d, \\ \Phi_A e^{-\xi y} & \text{if } y > \frac{1}{2}d, \end{cases} \tag{3-4}$$

for the symmetric modes in y , and

$$\phi_{as} = e^{i(\xi x - \omega t)} \begin{cases} \Phi_{A1} e^{\xi y} & \text{if } y < -\frac{1}{2}d, \\ \Phi_{B1} \sinh(\xi y) & \text{if } |y| \leq \frac{1}{2}d, \\ -\Phi_{A1} e^{-\xi y} & \text{if } y > \frac{1}{2}d, \end{cases} \tag{3-5}$$

for the antisymmetric modes in y , where Φ_A , Φ_B , Φ_{A1} , and Φ_{B1} are undetermined constants.

4. Dispersion relations

Now, the stress component $T \equiv T_{zy}$ and the electric displacement $D \equiv D_y$ are related to u and ϕ by

$$T = c \frac{\partial u}{\partial y} + e \frac{\partial \phi}{\partial y}, \quad D = e \frac{\partial u}{\partial y} - \varepsilon \frac{\partial \phi}{\partial y}. \tag{4-1}$$

It is convenient to express (4-1) using the potential function ϕ , which leads to the following expressions:

$$T = \bar{c} \frac{\partial u}{\partial y} + e \frac{\partial \phi}{\partial y}, \quad D = -\varepsilon \frac{\partial \phi}{\partial y}. \tag{4-2}$$

Substituting (3-1) and (3-4) into (2-3), the symmetric parts of the electric potential are written as

$$\varphi_s = e^{i(\xi x - \omega t)} \begin{cases} e_A/\varepsilon_A U_A e^{\eta_A y} + \Phi_A e^{\xi y} & \text{if } y < -\frac{1}{2}d, \\ e_B/\varepsilon_B U_B \cos(\eta_B y) + \Phi_B \cosh(\xi y) & \text{if } |y| \leq \frac{1}{2}d, \\ e_A/\varepsilon_A U_A e^{-\eta_A y} + \Phi_A e^{-\xi y} & \text{if } y > \frac{1}{2}d. \end{cases} \tag{4-3}$$

Substituting (3-1) and (3-4) into (4-2), we get the following expressions for the symmetric part of T and D :

$$T_s = e^{i(\xi x - \omega t)} \begin{cases} U_A \bar{c}_A \eta_A e^{\eta_A y} + \Phi_A \xi e^{\xi y} & \text{if } y < -\frac{1}{2}d, \\ -U_B \bar{c}_B \eta_B \sin(\eta_B y) + \Phi_B e_B \xi \sinh(\xi y) & \text{if } |y| \leq \frac{1}{2}d, \\ -U_A \bar{c}_A \eta_A e^{-\eta_A y} - \Phi_A e_A \xi e^{-\xi y} & \text{if } y > \frac{1}{2}d, \end{cases} \tag{4-4}$$

$$D_s = e^{i(\xi x - \omega t)} \begin{cases} -\Phi_A \varepsilon_A \xi e^{\xi y} & \text{if } y < -\frac{1}{2}d, \\ -\Phi_B \varepsilon_B \xi \sinh(\xi y) & \text{if } |y| \leq \frac{1}{2}d, \\ \Phi_A \varepsilon_A \xi e^{-\xi y} & \text{if } y > \frac{1}{2}d. \end{cases} \tag{4-5}$$

Analogously, we get the following expressions for the antisymmetric part of T and D :

$$T_{as} = e^{i(\xi x - \omega t)} \begin{cases} U_{A1} \bar{c}_A \eta_A e^{\eta_A y} + \Phi_{A1} \xi e^{\xi y} & \text{if } y < -\frac{1}{2}d, \\ U_{B1} \bar{c}_B \eta_B \cos(\eta_B y) + \Phi_{B1} e_B \xi \cosh(\xi y) & \text{if } |y| \leq \frac{1}{2}d, \\ U_{A1} \bar{c}_A \eta_A e^{-\eta_A y} + \Phi_{A1} e_A \xi e^{-\xi y} & \text{if } y > \frac{1}{2}d, \end{cases} \quad (4-6)$$

$$D_{as} = e^{i(\xi x - \omega t)} \begin{cases} -\Phi_{A1} \varepsilon_A \xi e^{\xi y} & \text{if } y < -\frac{1}{2}d, \\ -\Phi_{B1} \varepsilon_B \xi \cosh(\xi y) & \text{if } |y| \leq \frac{1}{2}d, \\ \Phi_{A1} \varepsilon_A \xi e^{-\xi y} & \text{if } y > \frac{1}{2}d. \end{cases} \quad (4-7)$$

4A. The symmetric part. Let us build the equations that satisfy the condition for the electro-mechanical imperfect contact at $y = -\frac{1}{2}d$ using the symmetric part of the solution. First,

$$T_A = k_u(u_A - u_B)$$

describes an elastic interface with spring constant material parameter $k_u > 0$. Then, we get

$$U_A(\bar{c}_A \eta_A - k_u) e^{-d\eta_A/2} + \Phi_A e_A \xi e^{-d\xi/2} + U_B k_u \cos(\frac{1}{2}d\eta_B) = 0, \quad (4-8)$$

with the second condition

$$T_B = k_u(u_A - u_B),$$

therefore we get

$$-U_A k_u e^{-d\eta_A/2} + U_B(\bar{c}_B \eta_B \sin(\frac{1}{2}d\eta_B) + k_u \cos(\frac{1}{2}d\eta_B)) - \Phi_B e_B \xi \sin(\frac{1}{2}d\xi) = 0. \quad (4-9)$$

The third condition,

$$D_A = k_\phi \left(\phi_A + \frac{e_A}{\varepsilon_A} u_A - \phi_B - \frac{e_B}{\varepsilon_B} u_B \right),$$

describes an electric interface with electric capacitor parameter $k_\phi > 0$, i.e., if the electric potential at the interface is discontinuous, we get

$$-\frac{e_A}{\varepsilon_A} U_A k_\phi e^{-d\eta_A/2} - \Phi_A k_\phi e^{-d\xi/2} + \frac{e_B}{\varepsilon_B} U_B k_\phi \cos(\frac{1}{2}d\eta_B) + \Phi_B k_\phi \cos(\frac{1}{2}d\xi) = 0. \quad (4-10)$$

Using the fourth condition,

$$D_B = k_\phi \left(\phi_A + \frac{e_A}{\varepsilon_A} u_A - \phi_B - \frac{e_B}{\varepsilon_B} u_B \right),$$

we obtain

$$-\frac{e_A}{\varepsilon_A} U_A k_\phi e^{-d\eta_A/2} - \Phi_A k_\phi e^{-d\xi/2} + \frac{e_B}{\varepsilon_B} U_B k_\phi \cos(\frac{1}{2}d\eta_B) + \Phi_B(\varepsilon_B \xi \sinh(\frac{1}{2}d\xi) + k_\phi \cosh(\frac{1}{2}d\xi)) = 0. \quad (4-11)$$

The set of equations (4-8)–(4-11) is a homogeneous system of linear algebraic equations for U_A , U_B , Φ_A , and Φ_B . In order to obtain nontrivial solutions, the determinant of the matrix formed by this system

of equations should be zero, and it can be simplified to

$$\begin{vmatrix} e_A \xi & 0 & \bar{c}_A \eta_A - k_u & k_u \cos(\frac{1}{2} d \eta_B) \\ 0 & -e_B \xi \sin(\frac{1}{2} d \xi) & -k_u & \bar{c}_B \eta_B \sinh(\frac{1}{2} d \eta_B) + k_u \cos(\frac{1}{2} d \eta_B) \\ -\varepsilon_A \xi - k_\varphi & k_\varphi \cosh(\frac{1}{2} d \xi) & -e_A / \varepsilon_A k_\varphi & e_B / \varepsilon_B k_\varphi \cos(\frac{1}{2} d \eta_B) \\ -k_\varphi & \varepsilon_B \xi \sinh(\frac{1}{2} d \xi) + k_\varphi \cosh(\frac{1}{2} d \xi) & -e_A / \varepsilon_A k_\varphi & e_B / \varepsilon_B k_\varphi \cos(\frac{1}{2} d \eta_B) \end{vmatrix}.$$

This determinant leads us to the following dispersion relations for the symmetric modes:

$$P_A P_B - Q^2 + k_u (P_A + P_B + 2Q) = 0,$$

where

$$\begin{aligned} P_A &= -\bar{c}_A \left(\eta_A - \xi \gamma_\varphi \frac{M_A^2}{\varepsilon_A} \right), & P_B &= \bar{c}_B \left(\eta_B \tan(\frac{1}{2} d \eta_B) + \xi \gamma_\varphi \frac{M_B^2}{\varepsilon_B} \right), \\ Q &= -\xi \gamma_\varphi \left(\frac{e_A e_B}{\varepsilon_A \varepsilon_B} \right), & \gamma_\varphi &= \frac{k_\varphi}{\xi + k_\varphi (1/\varepsilon_A + 1/\varepsilon_B \coth(\frac{1}{2} d \xi))}, \\ M_A^2 &= \frac{e_A^2}{\bar{c}_A \varepsilon_A}, & M_B^2 &= \frac{e_B^2}{\bar{c}_B \varepsilon_A}. \end{aligned}$$

4B. The antisymmetric part. We now build the equations that satisfy the condition for the electro-mechanical imperfect contact at $y = -\frac{1}{2}d$ using the antisymmetric part of the solution.

The first condition,

$$T_A = k_u (u_A - u_B),$$

describes an elastic interface with spring constant material parameter $k_u > 0$. Then, we get

$$U_{A1} (\bar{c}_A \eta_A - k_u) e^{-d \eta_A / 2} + \Phi_{A1} e_A \xi e^{-d \xi / 2} - U_{B1} k_u \sin(\frac{1}{2} d \eta_B) = 0. \tag{4-12}$$

With the second condition,

$$T_B = k_u (u_A - u_B),$$

we get

$$-U_{A1} k_u e^{-d \eta_A / 2} + U_{B1} (\bar{c}_B \eta_B \cos(\frac{1}{2} d \eta_B) - k_u \sin(\frac{1}{2} d \eta_B)) + \Phi_{B1} e_B \xi \cosh(\frac{1}{2} d \xi) = 0. \tag{4-13}$$

The third condition,

$$D_A = k_\varphi \left(\phi_A + \frac{e_A}{\varepsilon_A} u_A - \phi_B - \frac{e_B}{\varepsilon_B} u_B \right),$$

describes an electric interface with an electric capacitor parameter $k_\varphi > 0$, i.e., the electric potential at the interface must be discontinuous, so we obtain

$$-\frac{e_A}{\varepsilon_A} U_{A1} k_\varphi e^{-d \eta_A / 2} - \Phi_{A1} (\varepsilon_A \xi + k_\varphi) e^{-d \xi / 2} - \frac{e_B}{\varepsilon_B} U_{B1} k_\varphi \sin(\frac{1}{2} d \eta_B) - \Phi_{B1} k_\varphi \sinh(\frac{1}{2} d \xi) = 0. \tag{4-14}$$

Using the fourth condition,

$$D_B = k_\varphi \left(\phi_A + \frac{e_A}{\varepsilon_A} u_A - \phi_B - \frac{e_B}{\varepsilon_B} u_B \right),$$

we obtain,

$$\frac{e_A}{\varepsilon_A} U_{A1} k_\varphi e^{-d\eta_A/2} \Phi_{A1} k_\varphi e^{-d\xi/2} + \frac{e_B}{\varepsilon_B} U_{B1} k_\varphi \sin\left(\frac{1}{2}d\eta_B\right) + \Phi_{B1} \left(\varepsilon_B \xi \cosh\left(\frac{1}{2}d\xi\right) + k_\varphi \sinh\left(\frac{1}{2}d\xi\right) \right) = 0. \quad (4-15)$$

The set of equations (4-12)–(4-15) is a homogeneous system of linear algebraic equations for U_A , U_B , Φ_A , and Φ_B . In order to obtain nontrivial solutions, the determinant of the matrix formed by this system of equations should be zero, and it can be simplified to

$$\begin{vmatrix} e_A \xi & 0 & \bar{c}_A \eta_A - k_u & -k_u \sin\left(\frac{1}{2}d\eta_B\right) \\ 0 & e_B \xi \cosh\left(\frac{1}{2}d\xi\right) & -k_u & \bar{c}_B \eta_B \cos\left(\frac{1}{2}d\eta_B\right) - k_u \sin\left(\frac{1}{2}d\eta_B\right) \\ -\varepsilon_A \xi - k_\varphi & -k_\varphi \sinh\left(\frac{1}{2}d\xi\right) & -e_A/\varepsilon_A k_\varphi & -e_B/\varepsilon_B k_\varphi \sin\left(\frac{1}{2}d\eta_B\right) \\ -k_\varphi & -\varepsilon_B \xi \cosh\left(\frac{1}{2}d\xi\right) - k_\varphi \sinh\left(\frac{1}{2}d\xi\right) & -e_A/\varepsilon_A k_\varphi & -e_B/\varepsilon_B k_\varphi \sin\left(\frac{1}{2}d\eta_B\right) \end{vmatrix}.$$

This determinant leads us to the following dispersion relations for the antisymmetric modes:

$$P_A P_B - Q^2 + k_u(P_A + P_B + 2Q) = 0,$$

where

$$\begin{aligned} P_A &= -\bar{c}_A \left(\eta_A - \xi A \gamma_\phi \frac{M_A^2}{\varepsilon_A} \right), & P_B &= \bar{c}_B \left(\eta_B \tan\left(\frac{1}{2}d\eta_B\right) + \xi A \gamma_\phi \frac{M_B^2}{\varepsilon_B} \right), \\ Q &= -\xi A \gamma_\phi \left(\frac{e_A e_B}{\varepsilon_A \varepsilon_B} \right), & A \gamma_\phi &= \frac{k_\varphi}{\xi + k_\varphi (1/\varepsilon_A + 1/\varepsilon_B \tanh(\frac{1}{2}d\xi))}, \\ M_A^2 &= \frac{e_A^2}{\bar{c}_A \varepsilon_A}, & M_B^2 &= \frac{e_B^2}{\bar{c}_B \varepsilon_A}. \end{aligned}$$

5. Limit cases

Let us consider the following limit cases for the symmetric part:

(1) The interface has partial electrical interaction but has no mechanical interaction:

$$k_u \rightarrow 0, \quad 0 < k_\varphi < \infty,$$

$$\begin{aligned} \sqrt{1 - v^2/\bar{v}_A^2} \sqrt{v^2/\bar{v}_B^2 - 1} \tan\left(\frac{1}{2}d\xi \sqrt{v^2/\bar{v}_B^2 - 1}\right) + \gamma_\phi \frac{M_B^2}{\varepsilon_B} \sqrt{1 - v^2/\bar{v}_A^2} \\ - \gamma_\phi \frac{M_A^2}{\varepsilon_A} \sqrt{v^2/\bar{v}_B^2 - 1} \tan\left(\frac{1}{2}d\xi \sqrt{v^2/\bar{v}_B^2 - 1}\right) = 0. \end{aligned}$$

(2) The interface has perfect electrical interaction but has no mechanical interaction:

$$k_u \rightarrow 0, \quad k_\varphi \rightarrow \infty,$$

$$\begin{aligned} \sqrt{1 - v^2/\bar{v}_A^2} \sqrt{v^2/\bar{v}_B^2 - 1} \tan\left(\frac{1}{2}d\xi \sqrt{v^2/\bar{v}_B^2 - 1}\right) + \frac{M_B^2}{\varepsilon_B/\varepsilon_A + \coth\left(\frac{1}{2}d\xi\right)} \sqrt{1 - v^2/\bar{v}_A^2} \\ - \frac{M_A^2}{1 + \varepsilon_A/\varepsilon_B \coth\left(\frac{1}{2}d\xi\right)} \sqrt{v^2/\bar{v}_B^2 - 1} \tan\left(\frac{1}{2}d\xi \sqrt{v^2/\bar{v}_B^2 - 1}\right) = 0. \end{aligned}$$

(3) The interface has neither mechanical nor electrical interaction:

$$k_u \rightarrow 0, \quad k_\phi \rightarrow 0,$$

$$\sqrt{1 - v^2/\bar{v}_A^2} \sqrt{v^2/\bar{v}_B^2 - 1} \tan\left(\frac{1}{2}d\xi \sqrt{v^2/\bar{v}_B^2 - 1}\right) = 0 \rightarrow \sin\left(\frac{1}{2}d\xi \sqrt{v^2/\bar{v}_B^2 - 1}\right) = 0,$$

$$\frac{1}{4}d^2\xi^2(v^2/\bar{v}_B^2 - 1) = n^2\pi^2; \quad n \in \mathbb{Z}.$$

(4) The interface has perfect mechanical interaction but partial electrical interaction:

$$k_u \rightarrow \infty, \quad 0 < k_\phi < \infty,$$

$$\bar{c}_A \sqrt{1 - v^2/\bar{v}_A^2} - \bar{c}_B \sqrt{v^2/\bar{v}_B^2 - 1} \tan\left(\frac{1}{2}d\xi \sqrt{v^2/\bar{v}_B^2 - 1}\right) = \gamma_\phi (e_A/\varepsilon_A - e_B/\varepsilon_B)^2.$$

(5) The interface has both perfect mechanical and electrical interactions:

$$k_u \rightarrow \infty, \quad k_\phi \rightarrow \infty,$$

$$\bar{c}_A \sqrt{1 - v^2/\bar{v}_A^2} - \bar{c}_B \sqrt{v^2/\bar{v}_B^2 - 1} \tan\left(\frac{1}{2}d\xi \sqrt{v^2/\bar{v}_B^2 - 1}\right) = \frac{(e_A/\varepsilon_A - e_B/\varepsilon_B)^2}{1/\varepsilon_A + 1/\varepsilon_B \coth\left(\frac{1}{2}d\xi\right)}.$$

(6) The interface has perfect mechanical interaction but has no electrical interaction:

$$k_u \rightarrow \infty, \quad k_\phi \rightarrow 0,$$

$$\bar{c}_A \sqrt{1 - v^2/\bar{v}_A^2} - \bar{c}_B \sqrt{v^2/\bar{v}_B^2 - 1} \tan\left(\frac{1}{2}d\xi \sqrt{v^2/\bar{v}_B^2 - 1}\right) = 0.$$

Let us consider the following limit cases for the antisymmetric part:

(1) The interface has partial electrical interaction but has no mechanical interaction:

$$k_u \rightarrow 0, \quad 0 < k_\phi < \infty,$$

$$\sqrt{1 - v^2/\bar{v}_A^2} \sqrt{v^2/\bar{v}_B^2 - 1} \cot\left(\frac{1}{2}d\xi \sqrt{v^2/\bar{v}_B^2 - 1}\right) - A\gamma_\phi \frac{M_B^2}{\varepsilon_B} \sqrt{1 - v^2/\bar{v}_A^2}$$

$$- A\gamma_\phi \frac{M_A^2}{\varepsilon_A} \sqrt{v^2/\bar{v}_B^2 - 1} \cot\left(\frac{1}{2}d\xi \sqrt{v^2/\bar{v}_B^2 - 1}\right) = 0.$$

(2) The interface has perfect electrical interaction but has no mechanical interaction:

$$k_u \rightarrow 0, \quad k_\phi \rightarrow \infty,$$

$$\sqrt{1 - v^2/\bar{v}_A^2} \sqrt{v^2/\bar{v}_B^2 - 1} \cot\left(\frac{1}{2}d\xi \sqrt{v^2/\bar{v}_B^2 - 1}\right) - \frac{M_B^2}{\varepsilon_B/\varepsilon_A + \coth\left(\frac{1}{2}d\xi\right)} \sqrt{1 - v^2/\bar{v}_A^2}$$

$$- \frac{M_A^2}{1 + \varepsilon_A/\varepsilon_B \tanh\left(\frac{1}{2}d\xi\right)} \sqrt{v^2/\bar{v}_B^2 - 1} \cot\left(\frac{1}{2}d\xi \sqrt{v^2/\bar{v}_B^2 - 1}\right) = 0.$$

(3) The interface has neither mechanical nor electrical interaction:

$$k_u \rightarrow 0, \quad k_\phi \rightarrow 0,$$

$$\sqrt{1 - v^2/\bar{v}_A^2} \sqrt{v^2/\bar{v}_B^2 - 1} \cot\left(\frac{1}{2}d\xi \sqrt{v^2/\bar{v}_B^2 - 1}\right) = 0 \rightarrow \cos\left(\frac{1}{2}d\xi \sqrt{v^2/\bar{v}_B^2 - 1}\right) = 0,$$

$$d^2\xi^2(v^2/\bar{v}_B^2 - 1) = (2n + 1)^2\pi^2; \quad n \in \mathbb{Z}.$$

(4) The interface has perfect mechanical interaction but partial electrical interaction:

$$k_u \rightarrow \infty, \quad 0 < k_\phi < \infty,$$

$$\bar{c}_A \sqrt{1 - v^2/\bar{v}_A^2} + \bar{c}_B \sqrt{v^2/\bar{v}_B^2 - 1} \cot\left(\frac{1}{2}d\xi \sqrt{v^2/\bar{v}_B^2 - 1}\right) = A\gamma_\phi (e_A/\varepsilon_A - e_B/\varepsilon_B)^2.$$

(5) The interface has both perfect mechanical and electrical interactions:

$$k_u \rightarrow \infty, \quad k_\phi \rightarrow \infty,$$

$$\bar{c}_A \sqrt{1 - v^2/\bar{v}_A^2} - \bar{c}_B \sqrt{v^2/\bar{v}_B^2 - 1} \cot\left(\frac{1}{2}d\xi \sqrt{v^2/\bar{v}_B^2 - 1}\right) = \frac{(e_A/\varepsilon_A - e_B/\varepsilon_B)^2}{1/\varepsilon_A + 1/\varepsilon_B \tanh\left(\frac{1}{2}d\xi\right)}.$$

(6) The interface has perfect mechanical interaction but has no electrical interaction:

$$k_u \rightarrow \infty, \quad k_\phi \rightarrow 0,$$

$$\bar{c}_A \sqrt{1 - v^2/\bar{v}_A^2} - \bar{c}_B \sqrt{v^2/\bar{v}_B^2 - 1} \cot\left(\frac{1}{2}d\xi \sqrt{v^2/\bar{v}_B^2 - 1}\right) = 0.$$

6. Numerical examples

In order to show the effects of the imperfections within the interfaces, we present some dispersion curves. We used two different piezoelectric materials: BaTiO₃ as the piezoelectric A and PZT4 as the piezoelectric B. The properties of the materials are summarized in [Table 1](#).

In [Figure 2](#), dispersion curves $v = f(\omega d)$ for the symmetric part for the fixed electrical imperfect parameter $k_\phi = 0 \text{ F/m}^2$ and different values of the mechanical imperfect parameter k_u are shown. These curves are nonmonotonic for small values of k_u and strictly convex and decreasing for large values of k_u . As we can see, the dispersion curves are shifted to the right by increasing values of k_u . This behavior of the dispersion curves was shown by Otero et al. [[2011](#), Figures 2(a) and 2(b)]. The value of k_u has a really strong influence on the dispersion curves and all the wave velocities tend to the wave velocity in phase B as ωd goes to infinity. Nevertheless, for high frequencies, the wave propagation is not affected. The wave velocities are between v_A and v_B , and both are shown in [Figure 2](#).

In [Figure 3](#), dispersion curves for the symmetric part for $k_\phi = 5 \text{ F/m}^2$ and different values of the mechanical imperfect parameter k_u are shown. In [Figure 4](#), dispersion curves for the symmetric part for $k_\phi = 10^7 \text{ F/m}^2$ and different values of mechanical imperfect parameter k_u are shown.

The behavior in [Figures 3](#) and [4](#) are quite similar for the case $k_\phi = 0 \text{ F/m}^2$, but there is a slight difference, which is shown in [Figure 5](#), if we compare the dispersion curves for $k_u = 0.3 \text{ GPa/m}$ in all cases. As we

properties	BaTiO ₃	PZT4
c (GPa)	43	26
e (C/m ²)	11.6	10.5
ε (10 ⁻⁹ C ² /Nm ²)	11.2	7.124
ρ (10 ³ kg/m ³)	5	7.5
\bar{v} (10 ³ m/s)	3.07981	2.35162

Table 1. Material properties.

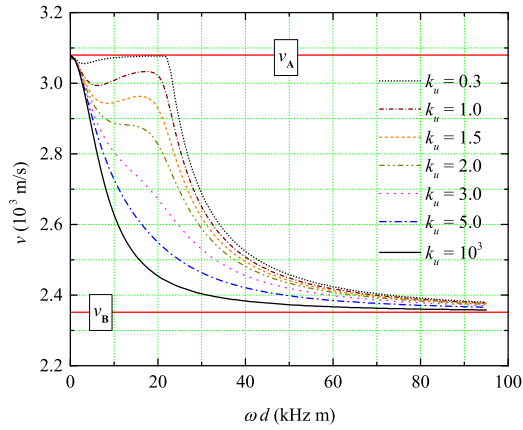


Figure 2. Dispersion curve for the symmetric part for $k_\varphi = 0 \text{ F/m}^2$ and different values of k_u .

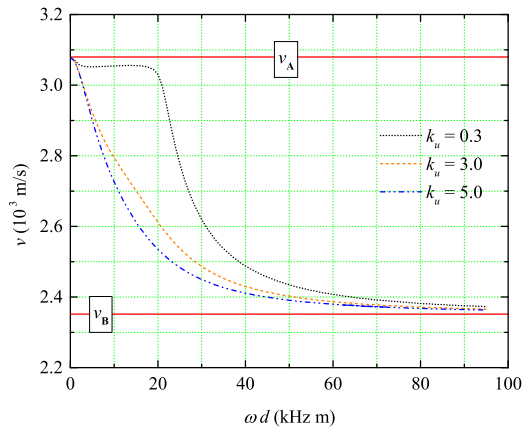


Figure 3. Dispersion curve for the symmetric part for $k_\varphi = 5 \text{ F/m}^2$ and different values of k_u .

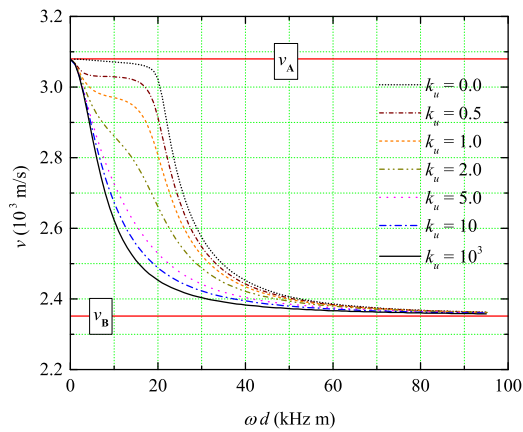


Figure 4. Dispersion curves for the symmetric part for $k_\varphi = 10^7 \text{ F/m}^2$ and different values of k_u .

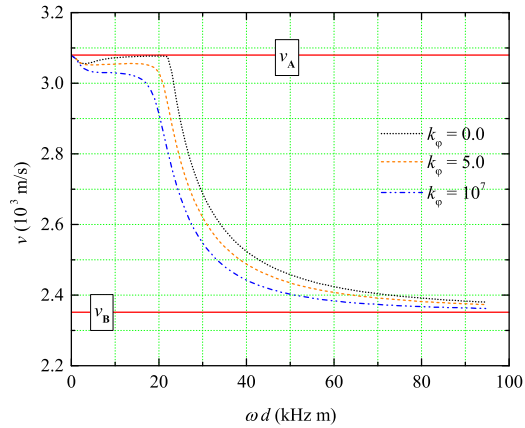


Figure 5. Dispersion curve for the symmetric part for $k_u = 0.3$ GPa/m and different values of k_φ .

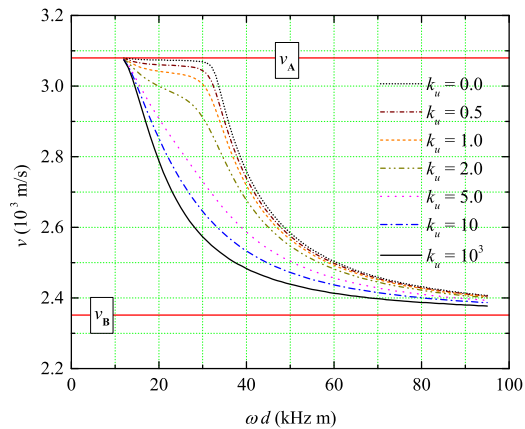


Figure 6. Dispersion curve for the antisymmetric part for $k_\varphi = 10$ F/m² and different values of k_u .

can see in [Figure 5](#), there is a notable displacement in both the frequency and the wave velocity axes. If k_φ is increased, the dispersion curves are shifted to the left and the wave velocity is decreased. This conclusion is really important because the dispersion curves are strongly dependent on the mechanical imperfect parameter (k_u) and depend weakly on the electrical parameter (k_φ).

In [Figure 6](#), dispersion curves for the antisymmetric part for the fixed electrical imperfect parameter $k_\varphi = 10$ F/m² and different values of mechanical imperfect parameter k_u are shown. These curves are strictly convex and have the same nonmonotonic behavior for small values for k_u and large values of k_u , similar to that of dispersion curves for the symmetric part. The visual difference between these curves and the symmetric ones is that dispersion curves for the antisymmetric part are shifted to the right. This behavior of the dispersion curves was shown in [[Otero et al. 2011](#), Figures 8(a) and 8(b)]. The value of k_u has a really strong influence in the dispersion curves and all the wave velocities approach to the wave velocity in phase B as ωd goes to infinity. Nevertheless, for high frequencies, the wave propagation is not affected. The wave velocities are between v_A and v_B , and both are shown in [Figure 6](#).

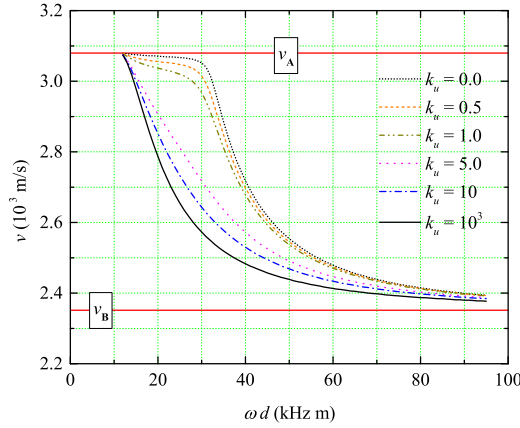


Figure 7. Dispersion curve for the antisymmetric part for $k_\varphi = 10^7 \text{ F/m}^2$ and different values of k_u .

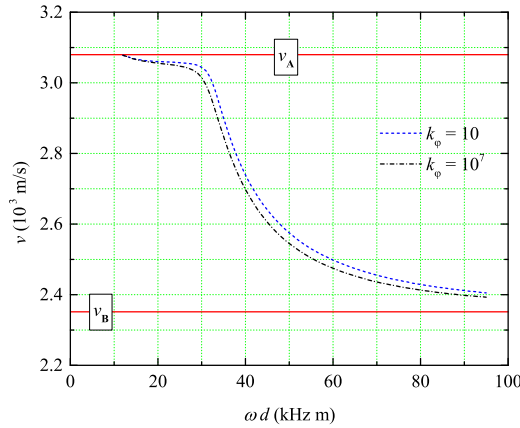


Figure 8. Dispersion curve for the antisymmetric part for $k_u = 0.5 \text{ GPa/m}$ and different values of k_φ .

In [Figure 7](#), dispersion curves for the antisymmetric part for $k_\varphi = 10^7 \text{ F/m}^2$ and different values of the mechanical imperfect parameter k_u are shown. The behavior in [Figures 6](#) and [7](#) are quite similar, but there is a slight difference, which is shown in [Figure 8](#), if we compare the dispersion curves for $k_u = 0.5 \text{ GPa/m}$ in both cases. As we can see in [Figure 8](#), there is a notable displacement in both the frequency and wave velocity axes, which is the same behavior as in the symmetric part.

7. Conclusions

Dispersion relations for the propagation of an interfacial shear wave in an A/B/A piezoelectric structure for symmetric and antisymmetric parts have been studied by considering the existence of electrical and mechanical imperfections at the interfaces, which are modeled by means a capacitor and a spring, respectively. Analytical expressions for dispersion relations are obtained and different limit cases are studied, showing a good agreement with [\[Otero et al. 2011\]](#). Numerical examples are presented by using two

piezoelectric materials (PZT4 and BaTiO₃), and dispersion curves for different values of the material parameters (k_u and k_ϕ) are shown. Some conclusions about dispersion curves have been obtained:

- they are confined within the velocity of media A and B for the symmetric and antisymmetric parts,
- they never intersect each other for the symmetric and antisymmetric parts,
- they go to v_B as ωd goes to infinity for all values of k_u , and possible values of k_ϕ ,
- they are nonmonotonic for small values for k_u , strictly convex and decreasing for large values of k_u ,
- the smaller the value of the imperfect bounding parameter (k_ϕ), the more shift to the right.

References

- [Bleustein 1968] J. L. Bleustein, “A new surface wave in piezoelectric materials”, *Appl. Phys. Lett.* **13**:12 (1968), 412–413.
- [Chen et al. 2008] Z. G. Chen, Y. T. Hu, and J. S. Yang, “Shear horizontal piezoelectric waves in a piezoceramic plate imperfectly bonded to two piezoceramic half-spaces”, *J. Mech.* **24**:3 (2008), 229–239.
- [Fan et al. 2006a] H. Fan, J. Yang, and L. Xu, “Antiplane piezoelectric surface waves over a ceramic half-space with an imperfectly bonded layer”, *IEEE Trans. Ultrason. Ferroelectr. Freq. Control* **53**:9 (2006), 1695–1698.
- [Fan et al. 2006b] H. Fan, J. Yang, and L. Xu, “Piezoelectric waves near an imperfectly bonded interface between two half-spaces”, *Appl. Phys. Lett.* **88**:20 (2006), 203509.
- [Kakar 2015] R. Kakar, “SH-wave velocity in a fiber-reinforced anisotropic layer overlying a gravitational heterogeneous half-space”, *Multi. Model. Mat. Struct.* **11**:3 (2015), 386–400.
- [Kong et al. 2016] Y. Kong, J. Liu, and G. Nie, “Propagation characteristics of SH waves in a functionally graded piezomagnetic layer on PMN-0.29PT single crystal substrate”, *Mech. Res. Commun.* **73** (2016), 107–112.
- [Li and Jin 2015] P. Li and F. Jin, “Excitation and propagation of shear horizontal waves in a piezoelectric layer imperfectly bonded to a metal or elastic substrate”, *Acta Mech.* **226**:2 (2015), 267–284.
- [Li et al. 2013] P. Li, F. Jin, W. Chen, and J. Yang, “Effects of interface bonding on acoustic wave generation in an elastic body by surface-mounted piezoelectric transducers”, *IEEE Trans. Ultrason. Ferroelectr. Freq. Control* **60**:9 (2013), 1957–1963.
- [Li et al. 2015a] Y.-D. Li, T. Xiong, and Q.-G. Cai, “Coupled interfacial imperfections and their effects on the fracture behavior of a layered multiferroic cylinder”, *Acta Mech.* **226**:4 (2015), 1183–1199.
- [Li et al. 2015b] Y.-D. Li, T. Xiong, and L. Dong, “A new interfacial imperfection coupling model (IICM) and its effect on the fracture behavior of a layered multiferroic composite: anti-plane case”, *Eur. J. Mech. A Solids* **52** (2015), 26–36.
- [Li et al. 2015c] Y.-D. Li, T. Xiong, and L. Dong, “Interfacial imperfection coupling model with application to the in-plane fracture problem of a multiferroic composite”, *Int. J. Solids Struct.* **54** (2015), 31–41.
- [Li et al. 2016a] Y.-D. Li, T. Xiong, and Y. Guan, “Effects of coupled interfacial imperfections on SH wave propagation in a layered multiferroic cylinder”, *Ultrasonics* **66** (2016), 11–17.
- [Li et al. 2016b] Y.-D. Li, K. Zhou, and T. Xiong, “Fracture analysis on a multiferroic cylindrical shell: effects of coupled interphase imperfections”, *J. Intell. Mater. Syst. Struct.* **27**:2 (2016), 195–207.
- [Liu et al. 2010] J. Liu, Y. Wang, and B. Wang, “Propagation of shear horizontal surface waves in a layered piezoelectric half-space with an imperfect interface”, *IEEE Trans. Ultrason. Ferroelectr. Freq. Control* **57**:8 (2010), 1875–1879.
- [Maerfeld and Tournois 1971] C. Maerfeld and P. Tournois, “Pure shear elastic surface wave guided by the interface of two semi-infinite media”, *Appl. Phys. Lett.* **19**:4 (1971), 117–118.
- [Otero et al. 2011] J. A. Otero, R. Rodríguez-Ramos, J. Bravo-Castillero, A. R. Aguiar, and G. Monsivais, “Dispersion relations for SH waves on a magneto-electroelastic heterostructure with imperfect interfaces”, *J. Mech. Mater. Struct.* **6**:7–8 (2011), 969–993.
- [Otero et al. 2012] J. A. Otero, R. Rodríguez-Ramos, J. Bravo-Castillero, and G. Monsivais, “Interfacial waves between two piezoelectric half-spaces with electro-mechanical imperfect interface”, *Philos. Mag. Lett.* **92**:10 (2012), 534–540.

- [Soh and Liu 2006] A. K. Soh and J. X. Liu, “Interfacial shear horizontal waves in a piezoelectric-piezomagnetic bi-material”, *Philos. Mag. Lett.* **86**:1 (2006), 31–35.
- [Sun et al. 2011] W.-H. Sun, G.-L. Ju, J.-W. Pan, and Y.-D. Li, “Effects of the imperfect interface and piezoelectric/piezomagnetic stiffening on the SH wave in a multiferroic composite”, *Ultrasonics* **51**:7 (2011), 831–838.
- [Xiong et al. 2015] T. Xiong, Y.-D. Li, and Z.-K. Song, “Interfacial sliding in a bi-layered multiferroic ceramics: localized sliding-prevention/promotion based mechanism of intra-layer fracture”, *Int. J. Solids Struct.* **77** (2015), 15–27.
- [Yang and Yang 2009] Z. Yang and J. Yang, “Effects of electric field gradient on the propagation of short piezoelectric interface waves”, *Int. J. Appl. Electrom.* **29**:2 (2009), 101–108.

Received 27 Nov 2016. Revised 22 Mar 2017. Accepted 29 Mar 2017.

M. A. REYES: 777marcorey@gmail.com

Instituto Politécnico Nacional, UPIITA-IPN, Avenida Instituto Politécnico Nacional No. 2580, Col Barrio la Laguna Ticomán, 07340 Ciudad de México., Mexico

J. A. OTERO: j.a.otero@itesm.mx

Campus Estado de México, Tecnológico de Monterrey, Carretera Lago de Guadalupe Km. 3.5, Atizapán de Zaragoza, 52926 Colonia Margarita Maza de Juárez., Mexico

R. PÉREZ-ÁLVAREZ: rpa@uaem.mx

Centro de Investigacion en Ciencias, Instituto de Investigacion en Ciencias Basicas y Aplicadas, Universidad Autonoma del Estado de Morelos, Av. Universidad 1001, 62209 Cuernavaca., Mexico

JOURNAL OF MECHANICS OF MATERIALS AND STRUCTURES

msp.org/jomms

Founded by Charles R. Steele and Marie-Louise Steele

EDITORIAL BOARD

ADAIR R. AGUIAR	University of São Paulo at São Carlos, Brazil
KATIA BERTOLDI	Harvard University, USA
DAVIDE BIGONI	University of Trento, Italy
YIBIN FU	Keele University, UK
IWONA JASIUK	University of Illinois at Urbana-Champaign, USA
MITSUTOSHI KURODA	Yamagata University, Japan
C. W. LIM	City University of Hong Kong
THOMAS J. PENCE	Michigan State University, USA
GIANNI ROYER-CARFAGNI	Università degli studi di Parma, Italy
DAVID STEIGMANN	University of California at Berkeley, USA
PAUL STEINMANN	Friedrich-Alexander-Universität Erlangen-Nürnberg, Germany

ADVISORY BOARD

J. P. CARTER	University of Sydney, Australia
D. H. HODGES	Georgia Institute of Technology, USA
J. HUTCHINSON	Harvard University, USA
D. PAMPLONA	Universidade Católica do Rio de Janeiro, Brazil
M. B. RUBIN	Technion, Haifa, Israel

PRODUCTION production@msp.org

SILVIO LEVY Scientific Editor


Cover photo: Mando Gomez, www.mandolux.com

See msp.org/jomms for submission guidelines.

JoMMS (ISSN 1559-3959) at Mathematical Sciences Publishers, 798 Evans Hall #6840, c/o University of California, Berkeley, CA 94720-3840, is published in 10 issues a year. The subscription price for 2017 is US \$615/year for the electronic version, and \$775/year (+\$60, if shipping outside the US) for print and electronic. Subscriptions, requests for back issues, and changes of address should be sent to MSP.

JoMMS peer-review and production is managed by EditFLOW[®] from Mathematical Sciences Publishers.

PUBLISHED BY

 **mathematical sciences publishers**
nonprofit scientific publishing

<http://msp.org/>

© 2017 Mathematical Sciences Publishers

B-splines collocation for plate bending eigenanalysis	CHRISTOPHER G. PROVATIDIS	353
Shear capacity of T-shaped diaphragm-through joints of CFST columns	BIN RONG, RUI LIU, RUOYU ZHANG, SHUAI LIU and APOSTOLOS FAFITIS	373
Polarization approximations for elastic moduli of isotropic multicomponent materials	DUC CHINH PHAM, NGUYEN QUYET TRAN and ANH BINH TRAN	391
A nonlinear micromechanical model for progressive damage of vertebral trabecular bones	EYASS MASSARWA, JACOB ABOUDI, FABIO GALBUSERA, HANS-JOACHIM WILKE and RAMI HAJ-ALI	407
Nonlocal problems with local Dirichlet and Neumann boundary conditions	BURAK AKSOYLU and FATIH CELIKER	425
Optimization of Chaboche kinematic hardening parameters by using an algebraic method based on integral equations	LIU SHIJIE and LIANG GUOZHU	439
Interfacial waves in an A/B/A piezoelectric structure with electro-mechanical imperfect interfaces	M. A. REYES, J. A. OTERO and R. PÉREZ-ÁLVAREZ	457
Fully periodic RVEs for technological relevant composites: not worth the effort!	KONRAD SCHNEIDER, BENJAMIN KLUSEMANN and SWANTJE BARGMANN	471
Homogenization of a Vierendeel girder with elastic joints into an equivalent polar beam	ANTONIO GESUALDO, ANTONINO IANNUZZO, FRANCESCO PENTA and GIOVANNI PIO PUCILLO	485
Highly accurate noncompatible generalized mixed finite element method for 3D elasticity problems	GUANGHUI QING, JUNHUI MAO and YANHONG LIU	505
Thickness effects in the free vibration of laminated magneto-electroelastic plates	CHAO JIANG and PAUL R. HEYLIGER	521
Localized bulging of rotating elastic cylinders and tubes	JUAN WANG, ALI ALTHOBAITI and YIBIN FU	545